NEAR-BOTTOM CURRENTS ON THE MIDDLE SHOREFACE IN THE PRESENCE OF THE RHINE RIVER PLUME

Martijn Henriquez[1], Saulo Meirelles[2], Alexander R. Horner-Devine[3], Alejandro J. Souza[4], Julie D. Pietrzak[5], Marcel J.F. Stive[6]

The South-Holland coast of the Netherlands undergoes the influence of the Rhine river plume released from the Rotterdam waterways. An experiment, STRAINS, was conducted to study the impact of the fresh water on the nearshore hydrodynamics and sand transport. As part of the experiment, an instrumented bottom frame measured the near-bed hydrodynamics at 12 m depth. The flow was decomposed in the tidal, wave and turbulent component. During moderate energetic wave conditions the cross-shore tidal flow was of similar magnitude as the wave orbital flow. The cross-shore tidal flow was asymmetric and larger in the seaward direction. The cross-shore tidal component may be generated by tidal straining due to the river plume.

Keywords: field measurements; lower shoreface; tidal straining; sediment transport

INTRODUCTION

The Rhine River flows out into the North Sea near the Port of Rotterdam and the river plume creates a Region Of Freshwater Influence (ROFI) along the coast of The Netherlands (De Boer et al., 2006). This area was the site of the recent STRAINS experiment (STRAtification Impacts on Nearshore Sediment transport) (Horner-Devine, in prep.). The study region was located approx. 10 km to the North of the Port of Rotterdam at the Sand Engine nourishment (Stive et al., 2013). See Figure 1 for an overview of the area. The Rhine ROFI plays a key role in the hydrodynamic circulation along the coast and the water column (Souza and Simpson, 1996). The release of fresh river water generates stratification. In combination with the tide, this causes tidal straining and cross-shore velocity shear (De Boer et al., 2006). The impact of these cross-shore currents on sand transport is unknown and was investigated by conducting field measurements.

As part of the STRAINS experiment, an instrumented bed-frame, named the NEMO lander, was deployed at -12 m NAP (Dutch datum at approx. mean sea level) in February 2013 for 21 days. Current profiles were estimated from a downward-looking ADCP (Nortek Aquadopp HR) mounted 50 cm above the bed. Current profiles throughout the water column were recorded from an upward-looking ADCP (Nortek Aquadopp). Near-bottom flow velocities were also measured with two ADVs (Nortek Vector) positioned 0.56 m above the bed and sampled with 8 Hz. The ADVs measured one after another with an overlap of 6 days. Other instruments (CTD, OBS, ADCP, LISST) were mounted on two additional frames and two additional moorings. Those measurement are not analyzed in this paper.

In this paper we focus on ADV measurements during the overlap period of 6 days. During this period the offshore wave height H_s ranged between 0.5-1.4 m traveling from the northward direction. Salinity measurements indicated that the vertical water column was stratified and the density ranged from 1020 – 1025 kg/m^3. The aim of this paper is to separate the flow velocity in the tidal $\breve{u}$, wave $\tilde{u}$ and turbulent u' components. The time overlap allows for the separation of the wave orbital velocity from the measured velocities using the method described by (Shaw and Trowbridge, 2001).

METHODOLOGY

Tidal component

The time series was divided in consecutive windows of 10 minutes. The tidal component was determined by averaging over a consecutive window of 10 minutes:

$$\breve{u}(m) = \frac{1}{k}\left[u(1+(n-1)k) + u(2+(n-1)k) + \ldots + u(nk)\right] \tag{1}$$

where m is the mth discrete sample, n is the window counter and k is equal to the number of samples in a window, i.e. $k = 10 \times 60 \times 8$. Note that by definition $\breve{u}(m)$ is constant within the window. The tidal

[1]Department of Hydraulic Engineering, Delft University of Technology, Netherlands, m.henriquez@tudelft.nl
[2]Department of Hydraulic Engineering, Delft University of Technology, Netherlands, s.meirellesnunesdarocha@tudelft.nl
[3]Civil & Environmental Engineering, University of Washington,Seattle, Washington, USA, arhd@u.washington.edu
[4]National Oceanography Center, Joseph Proudman Building, Liverpool, UK, ajso@noc.ac.uk
[5]Department of Hydraulic Engineering, Delft University of Technology, Netherlands, j.d.pietrzak@tudelft.nl
[6]Department of Hydraulic Engineering, Delft University of Technology, Netherlands, m.j.f.stive@tudelft.nl

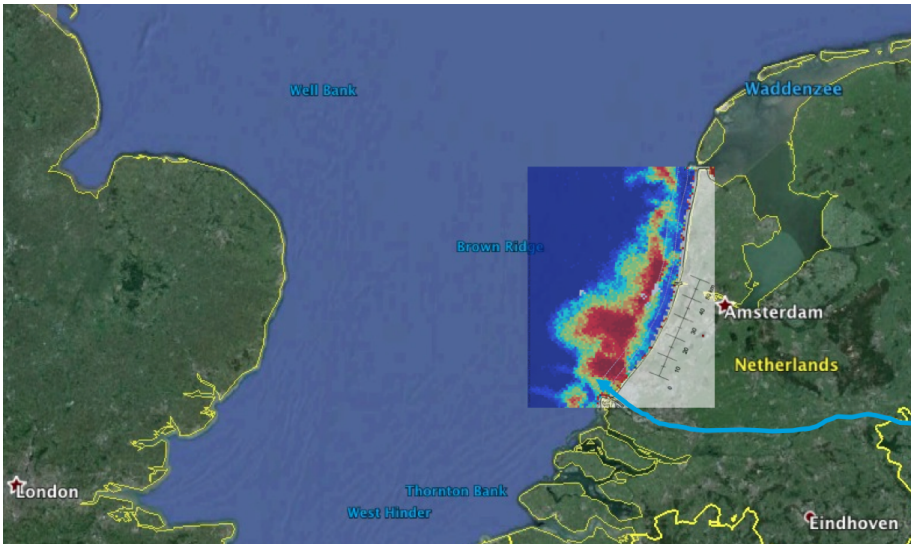

Figure 1: Google earth image of the North Sea including the South-Holland coast on the right. The inset shows the sea surface temperature where red color indicates higher temperatures (source: NOAA). The blue line represents the Rhine river.

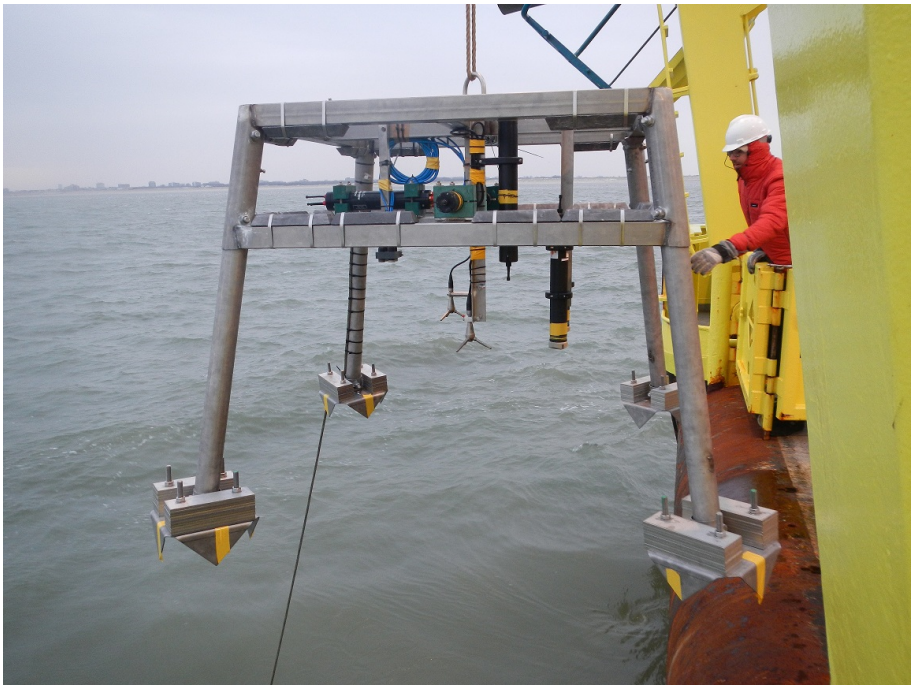

Figure 2: Deployment of the NEMO lander.

component was subtracted from the 10 minute windows of the time series resulting in the combined wave and turbulent components:

$$\tilde{u}(t) + u'(t) = u(t) - \breve{u}(t) \quad . \tag{2}$$

Wave and turbulent component

The method described by (Shaw and Trowbridge, 2001) works when the wave motion between the ADVs was coherent and the turbulence was not coherent. The velocity u_2 of the second ADV was used to estimate the wave component $\tilde{u}_{1,EST}$ at the first ADV. A transversal filter $h(m)$ was applied that represents the relation between the wave components $\tilde{u}_1$ and $\tilde{u}_2$ of the two ADVs. The weights of the filter $h(t)$ were

estimated by finding the ordinary least squares solution of $\mathbf{A}h = u_1$. The matrix $\mathbf{A}$ was an $M \times N$ matrix of velocity u_2 where M was the number of samples and N the (uneven) number of filter weights. The matrix had the form:

$$\left[u_2\left(m - \frac{N-1}{2}\right), \ldots, u_2(m), \ldots, u_2\left(m + \frac{N-1}{2}\right)\right] \quad . \tag{3}$$

The number of weights was approx. equal to the number of samples that constitute the peak wave period T_p. By multiplying the matrix with the filter weights, the wave velocity $\tilde{u}_{1,EST}$ at the first ADV was estimated:

$$\tilde{u}_{1,EST} = \mathbf{A}h \tag{4}$$

and consequently the turbulent component was estimated:

$$u'_{1,EST} = u_1 - \tilde{u}_{1,EST} \quad . \tag{5}$$

Furthermore, the root-mean-square wave component $\tilde{u}_{RMS}$ was determined by averaging over the 10 min window; similar for the turbulent component u'_{RMS}. The analysis resulted in an $\breve{u}$, $\tilde{u}_{RMS}$ and u'_{RMS} for every consecutive 10 min window.

RESULTS

Figure 3 shows the flow components during the overlap period. The alongshore tidal velocity was 0.5 m/s in the northeast direction, coinciding with the propagating direction of the tidal wave, and 0.4 m/s in the southwest direction. The cross-shore tidal velocity was significantly larger in the seaward direction than in the shoreward direction. While the shoreward magnitudes ranged between 0-0.1 m/s, the seaward magnitudes were around 0.2 m/s. The cross-shore root-mean-square wave velocities $\tilde{u}_{RMS}$ peaked just above 0.1 m/s during the more energetic wave conditions. The cross-shore root-mean-square turbulent velocities followed the alongshore tidal velocities and were not larger than $u'_{RMS} \leq 0.05$ m/s.

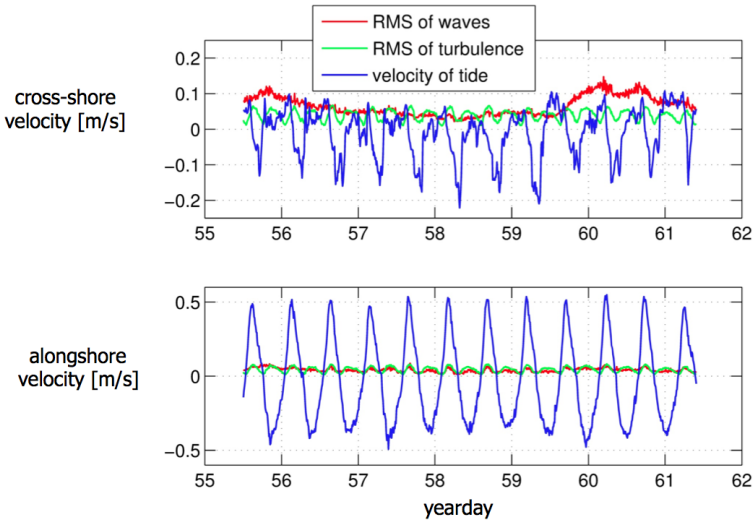

Figure 3: Cross-shore velocities (negative values mean offshore flow) in the upper panel and alongshore velocities (negative values mean southward flow) in the lower panel.

CONCLUSION

During the ADV overlap period, the alongshore tidal velocity $\breve{v}$ was dominant even during wave heights of $H_s = 1.4$ m. However, the cross-shore wave velocity $\tilde{u}$ was of the same order of magnitude as the tidal velocity.

The cross-shore tidal velocity $\breve{u}$ was twice as large as the cross-shore root-mean-square wave velocity $\tilde{u}_{RMS}$. Since the cross-shore tidal velocity $\breve{u}$ was mainly directed seawards, it could be an important driver for the seaward (offshore) sediment transport.

It may be that the cross-shore tidal velocities $\breve{u}$ were generated by tidal straining. Further investigation is suggested to relate tidal straining, cross-shore tidal velocities and cross-shore sediment transport.

AKNOWLEDGEMENT

The authors would like to thank the ERC and STW for funding this research through the NEMO and Sustainable ROFIs project. The authors are indebted to Ad Stolk from Rijkswaterstaat for providing the M/V Arca and its crew for the deployment of instruments. We also wish to thank Wil Borst, Onno van Tongeren from the Port of Rotterdam for their support and NIOZ for instruments. Alejandro Souza was supported by NERC-NC through direct funding to NOC.

REFERENCES

G. J. De Boer, J. D. Pietrzak, and J. C. Winterwerp. On the vertical structure of the rhine region of freshwater influence. *Ocean dynamics*, 56(3-4):198–216, 2006.

W. J. Shaw and J. H. Trowbridge. The direct estimation of near-bottom turbulent fluxes in the presence of energetic wave motions. *Journal of Atmospheric and Oceanic Technology*, 18(9):1540–1557, 2001.

A. Souza and J. Simpson. The modification of tidal ellipses by stratification in the rhine rofi. *Continental Shelf Research*, 16(8):997–1007, July 1996. URL `http://nora.nerc.ac.uk/503315/`.

M. J. F. Stive, M. A. de Schipper, A. P. Luijendijk, S. G. J. Aarninkhof, C. van Gelder-Maas, J. S. M. van Thiel de Vries, S. de Vries, M. Henriquez, S. Marx, and R. Ranasinghe. A new alternative to saving our beaches from sea-level rise: The sand engine. *Journal of Coastal Research*, 29(5):1001–1008, 2013.